Observability Investigation for Rotational Calibration of (Global-pose aided) VIO under Straight Line Motion

Supplementary Material

VII. Correction of the observability matrix for global-pose aided VIO

The observability matrix plays a key role for the observability analysis of a linear or nonlinear state estimator. According to the Section II.E of [19], the measurement Jacobian matrix and state transition matrix need to be calculated in advance to construct the observability matrix. For ease of description, recall our state vector (Eq. (1))

$$x = \begin{bmatrix} {}^{I}_{G}q^T & b_g^T & {}^{G}v_I^T & b_a^T & {}^{G}p_I^T & {}^{C}_{I}q^T & {}^{G}p_f^T \end{bmatrix}^T \quad (23)$$

According to the Section II.D of [19], the measurement Jacobian matrix corresponding to global pose measurement can be calculated as

$$H_{V_k} = \begin{bmatrix} I_3 & 0_3 & 0_3 & 0_3 & 0_3 & 0_3 & 0_3 \\ 0_3 & 0_3 & 0_3 & 0_3 & I_3 & 0_3 & 0_3 \end{bmatrix} \quad (24)$$

Combining the measurement Jacobian matrix corresponding to visual measurement, H_{C_k}, the overall measurement Jacobian matrix can be denoted as

$$H_k = \begin{bmatrix} H_{C_k} \\ H_{V_k} \end{bmatrix} \quad (25)$$

Referring to equation (5) of [19], the expression of our state transition matrix is

$$\Phi(k,1) = \begin{bmatrix} \Phi_{I11} & \Phi_{I12} & 0_3 & 0_3 & 0_3 & 0_3 & 0_3 \\ 0_3 & I_3 & 0_3 & 0_3 & 0_3 & 0_3 & 0_3 \\ \Phi_{I31} & \Phi_{I32} & I_3 & \Phi_{I34} & 0_3 & 0_3 & 0_3 \\ 0_3 & 0_3 & 0_3 & I_3 & 0_3 & 0_3 & 0_3 \\ \Phi_{I51} & \Phi_{I52} & \Phi_{I53} & \Phi_{I54} & I_3 & 0_3 & 0_3 \\ 0_3 & 0_3 & 0_3 & 0_3 & 0_3 & I_3 & 0_3 \\ 0_3 & 0_3 & 0_3 & 0_3 & 0_3 & 0_3 & I_3 \end{bmatrix} \quad (26)$$

Finally, the observability matrix for global-pose aided VIO can be constructed by multiplying the measurement Jacobian matrix with the state transition matrix

$$\begin{aligned} M_k^{(g)} &= H_k \Phi(k,1) \\ &= \begin{bmatrix} H_{C_k}\Phi(k,1) \\ H_{V_k}\Phi(k,1) \end{bmatrix} \\ &= \begin{bmatrix} \Xi_k \Xi_{\Gamma_k} \\ H_{V_k}\Phi(k,1) \end{bmatrix} \\ &= \begin{bmatrix} \Xi_k & 0 \\ 0 & I_6 \end{bmatrix} \\ &\quad \times \begin{bmatrix} \Gamma_1 & \Gamma_2 & -I_3\delta t_k & \Gamma_3 & -I_3 & \Gamma_4 & I_3 \\ \Phi_{I11} & \Phi_{I12} & 0_3 & 0_3 & 0_3 & 0_3 & 0_3 \\ \Phi_{I51} & \Phi_{I52} & \Phi_{I53} & \Phi_{I54} & I_3 & 0_3 & 0_3 \end{bmatrix} \end{aligned} \quad (27)$$

This completes the correction for the equation (40) of [19].

VIII. Additional results on numerical study

In this section, we will analyze additional calibration results described in Tab. III to complete the validation of our observable conclusions.

Tab. VI shows the final calibration results of Trajectory-1 in the global-pose aided VIO configuration. For Case-1, pitch and yaw exhibit observable characteristic, while roll not. This is because the non-zero component of ${}^{C}_{I}Rd$ corresponds to roll. For Case-2, yaw exhibits observable characteristic, while roll and pitch not. This is because non-zero components of ${}^{C}_{I}Rd$ correspond to roll and pitch. For Case-3, roll, pitch, and yaw all exhibit unobservable characteristic. This is because none of the three components of ${}^{C}_{I}Rd$ are zero. The calibration results over time are shown in the Fig. 7.

Tab. VII shows the final calibration results of Trajectory-2 in the pure VIO configuration. For Case-1, Case-2, and Case-3, roll, pitch, and yaw all exhibit unobservable characteristic. This can be explained by Lemma 2, which indicates constant velocity motion lead to the fully unobservable property of the rotational extrinsic parameter. The calibration results over time are shown in the Fig. 8.

Tab. VIII shows the final calibration results of Trajectory-2 in the global-pose aided VIO configuration. We can still observe that the convergence of the rotational extrinsic parameter, depends on which components of ${}^{C}_{I}Rd$ are 0. The calibration results over time are shown in the Fig. 9.

These calibration results, and the corresponding observability conclusion they supported, are summarized in Tab. III. Extensive experimental results demonstrate the correctness of our novel theoretical finding (see Tab. I).

TABLE VI: Final calibration results of the rotational extrinsic parameter for global-pose aided VIO system undergoes pure translational straight line motion with variable velocity. The absolute errors of roll, pitch, and yaw at 60s, are recorded with different perturbations.

Perturbations of (roll, pitch, yaw)	Case-1			Case-2			Case-3		
	Roll	Pitch	Yaw	Roll	Pitch	Yaw	Roll	Pitch	Yaw
(2, -4, -5)	0.89	0.07	0.01	4.00	1.73	0.02	4.98	1.84	2.15
(-4, 3, 3)	12.49	0.08	0.01	9.44	3.98	0.12	0.89	0.28	0.37
(5, -2, -1)	1.22	0.08	0.01	1.05	0.50	0.01	7.34	2.71	3.21
(-1, -5, -3)	5.82	0.08	0.01	6.82	2.89	0.06	3.62	1.33	1.55
(3, 0, 1)	4.31	0.08	0.01	2.87	1.26	0.02	6.01	2.22	2.62
(1, 2, -4)	5.33	0.08	0.01	4.83	2.07	0.03	2.92	1.06	1.25
(0, 5, 2)	8.68	0.08	0.01	5.59	2.39	0.05	2.98	1.08	1.29
(-3, 4, 0)	10.75	0.08	0.01	8.53	3.60	0.10	1.28	0.43	0.53
(-5, 1, 4)	13.39	0.08	0.01	10.38	4.37	0.14	0.92	0.29	0.38
(4, -1, 5)	4.49	0.08	0.01	1.88	0.85	0.01	8.02	2.96	3.52
(-2, -3, -2)	7.50	0.08	0.01	7.80	3.30	0.08	3.23	1.18	1.38
Avg	6.81	0.08	0.01	5.74	2.45	0.06	3.84	1.40	1.66

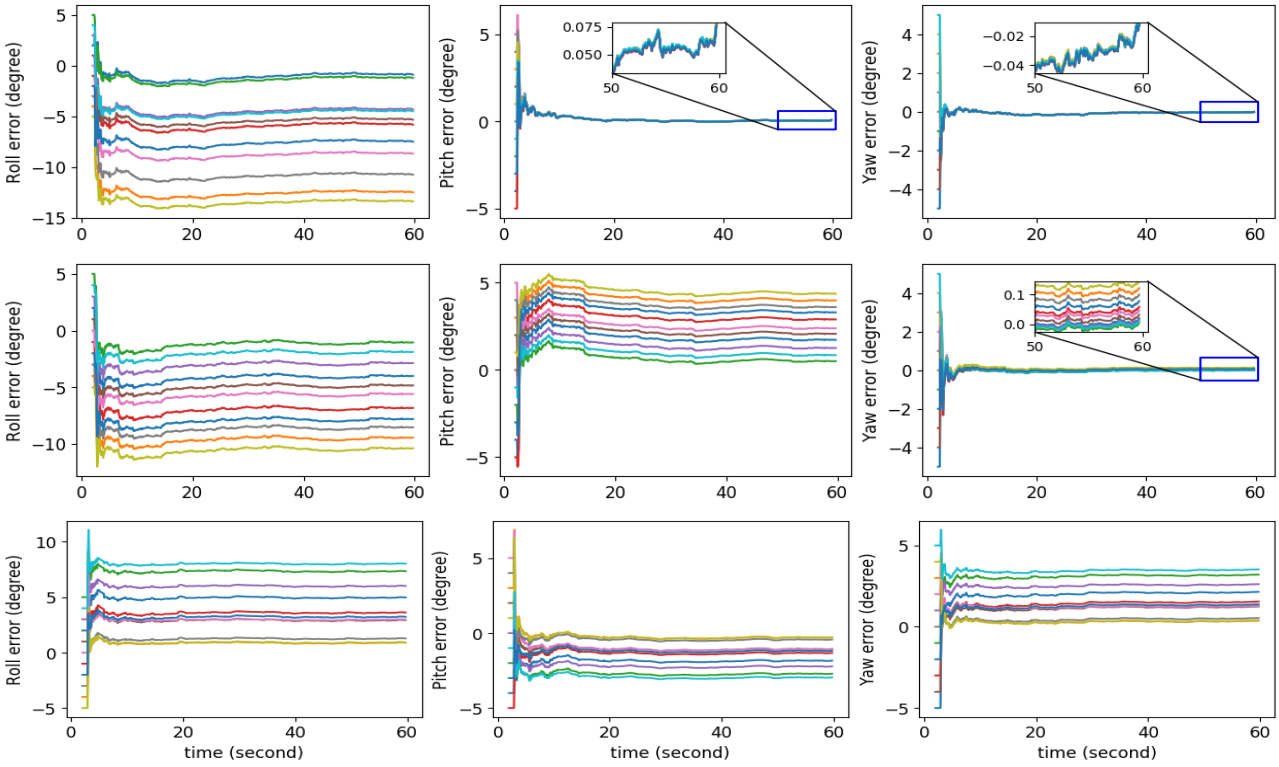

Fig. 7: Calibration results for global-pose aided VIO system undergoes pure translational straight line motion with variable velocity. y-axis represents errors of the rotational calibration parameter over time respect to different initial guesses. x-axis represents time in seconds. Top to bottom corresponds to Case-1 to Case-3 in Sec. V-B.

TABLE VII: Final calibration results of the rotational extrinsic parameter for pure VIO system undergoes pure translational straight line motion with constant velocity. The absolute errors of roll, pitch, and yaw at 60s, are recorded with different perturbations.

Perturbations of (roll, pitch, yaw)	Case-1			Case-2			Case-3		
	Roll	Pitch	Yaw	Roll	Pitch	Yaw	Roll	Pitch	Yaw
(2, -4, -5)	0.46	5.65	4.81	4.63	3.70	2.06	1.29	10.38	4.34
(-4, 3, 3)	2.77	1.82	3.77	7.74	2.02	2.03	5.97	2.39	6.96
(5, -2, -1)	5.40	6.66	1.41	7.18	3.41	0.20	21.48	10.81	1.41
(-1, -5, -3)	2.40	6.27	2.12	0.61	2.73	0.27	0.72	2.23	0.53
(3, 0, 1)	5.02	6.24	0.77	3.21	0.99	0.94	7.66	16.23	4.27
(1, 2, -4)	0.13	4.23	4.48	3.18	0.37	2.77	6.71	10.27	3.55
(0, 5, 2)	0.86	0.99	2.97	2.20	1.87	1.18	2.39	11.00	6.96
(-3, 4, 0)	1.63	3.45	0.41	3.57	2.04	0.25	2.33	3.93	1.67
(-5, 1, 4)	3.36	2.93	4.19	8.86	2.06	3.06	5.93	0.16	9.01
(4, -1, 5)	5.83	3.71	4.64	1.12	1.61	4.09	10.51	8.93	11.47
(-2, -3, -2)	2.57	6.09	1.25	0.77	1.56	0.17	2.92	2.72	1.42
Avg	2.77	4.37	2.80	3.91	2.03	1.55	6.17	7.19	4.69

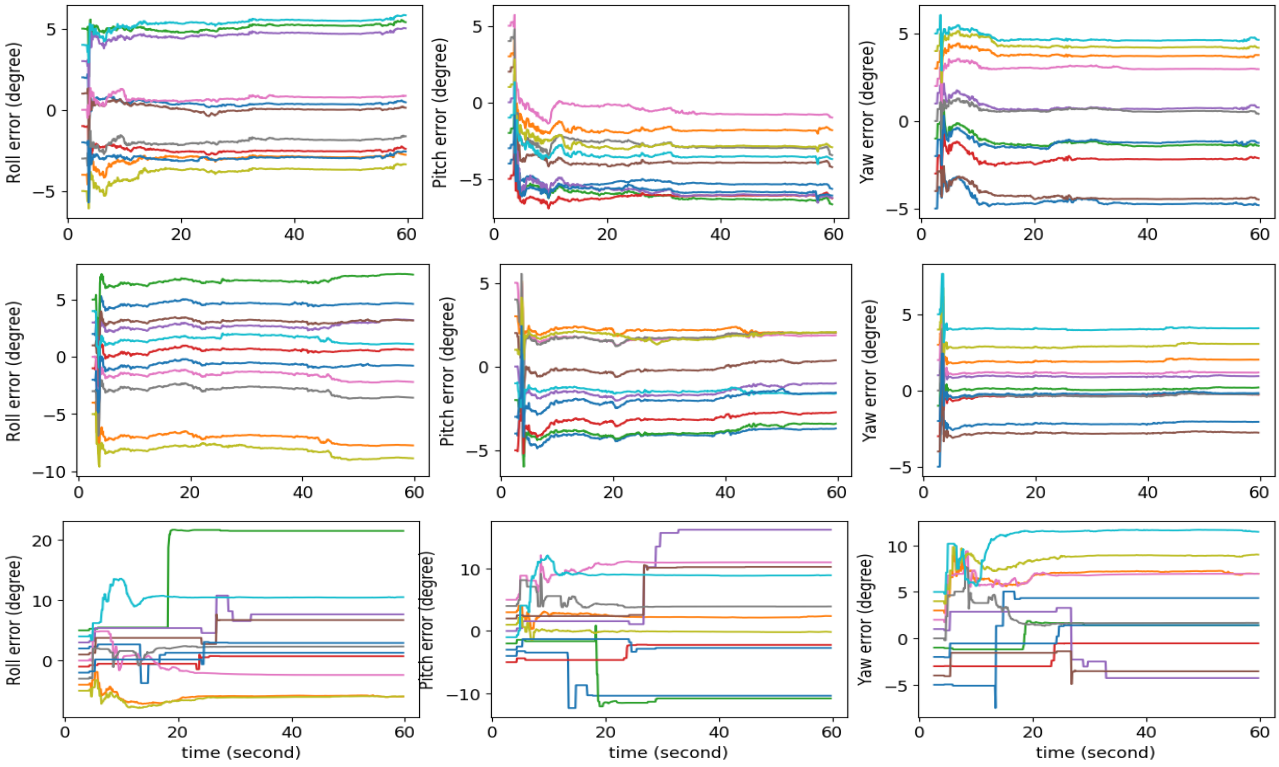

Fig. 8: Calibration results for pure VIO system undergoes pure translational straight line motion with constant velocity. y-axis represents errors of the rotational calibration parameter over time respect to different initial guesses. x-axis represents time in seconds. Top to bottom corresponds to Case-1 to Case-3 in Sec. V-B.

TABLE VIII: Final calibration results of the rotational extrinsic parameter for global-pose aided VIO system undergoes pure translational straight line motion with constant velocity. The absolute errors of roll, pitch, and yaw at 60s, are recorded with different perturbations.

Perturbations of (roll, pitch, yaw)	Case-1			Case-2			Case-3		
	Roll	Pitch	Yaw	Roll	Pitch	Yaw	Roll	Pitch	Yaw
(2, -4, -5)	1.90	0.01	0.01	4.38	1.83	0.01	0.30	0.13	0.11
(-4, 3, 3)	4.56	0.00	0.02	2.39	1.00	0.00	8.82	3.22	3.90
(5, -2, -1)	1.88	0.00	0.01	6.66	2.76	0.03	9.69	3.57	4.22
(-1, -5, -3)	4.39	0.01	0.00	2.25	0.95	0.02	4.42	1.67	1.84
(3, 0, 1)	0.70	0.00	0.01	4.33	1.79	0.01	9.39	3.48	4.11
(1, 2, -4)	1.07	0.00	0.00	2.45	1.02	0.03	4.05	1.52	1.76
(0, 5, 2)	0.09	0.01	0.01	0.56	0.22	0.01	6.75	2.53	2.95
(-3, 4, 0)	3.47	0.01	0.01	1.46	0.61	0.01	4.06	1.52	1.76
(-5, 1, 4)	6.06	0.00	0.02	2.67	1.12	0.01	9.84	3.58	4.33
(4, -1, 5)	1.60	0.00	0.02	4.82	1.98	0.03	14.31	5.16	6.35
(-2, -3, -2)	4.78	0.01	0.01	0.96	0.41	0.02	2.50	0.93	1.04
Avg	2.77	0.01	0.01	2.99	1.24	0.02	6.74	2.48	2.94

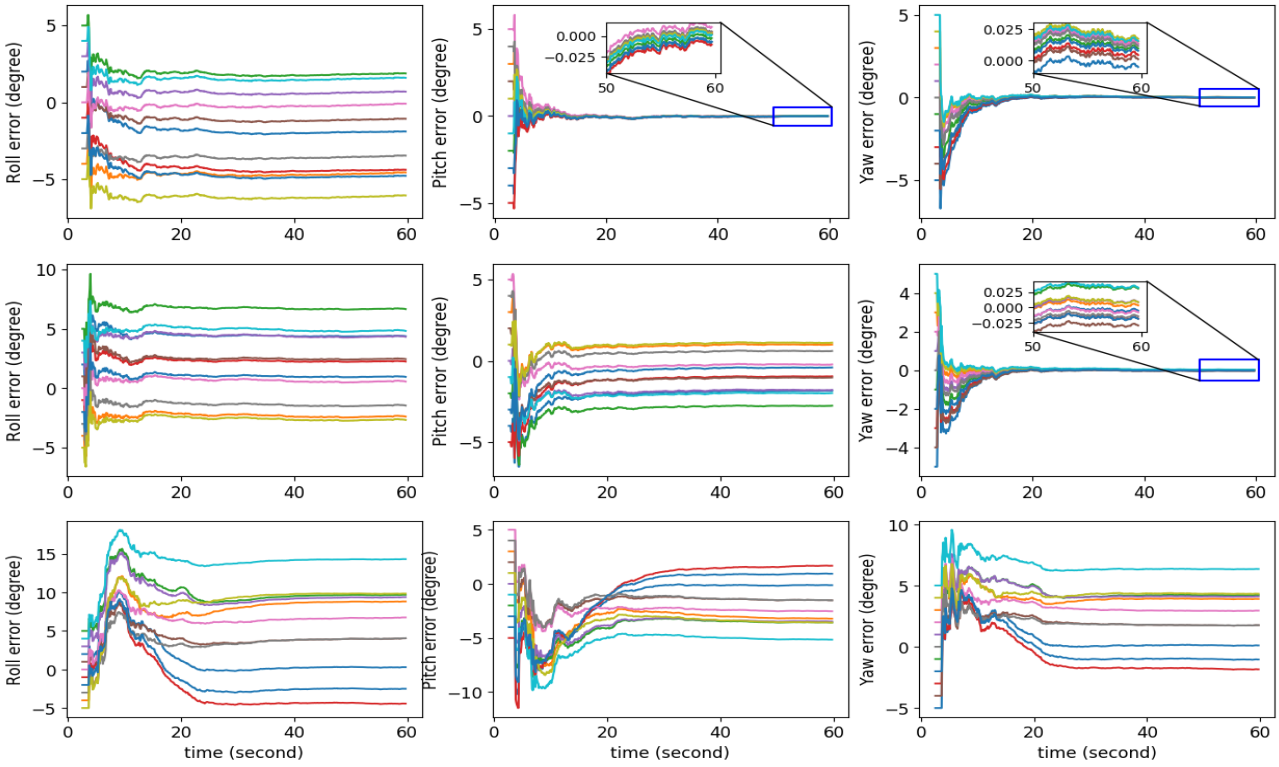

Fig. 9: Calibration results for global-pose aided VIO system undergoes pure translational straight line motion with constant velocity. y-axis represents errors of the rotational calibration parameter over time respect to different initial guesses. x-axis represents time in seconds. Top to bottom corresponds to Case-1 to Case-3 in Sec. V-B.